Global and Planetary Change 201 (2021) 103479

Contents lists available at ScienceDirect

Global and Planetary Change

journal homepage: www.elsevier.com/locate/gloplacha

Growing at the limit: Reef growth sensitivity to climate and oceanographic changes in the South Western Atlantic

Guilherme H. Pereira-Filho [a,*], Vinícius R. Mendes [a], Chris T. Perry [b], Gustavo I. Shintate [a], Willians C. Niz [a], André O. Sawakuchi [c], Alex C. Bastos [d], Paulo César F. Giannini [c], Fabio S. Motta [a], Christian Millo [e], Gustavo M. Paula-Santos [f], Rodrigo L. Moura [g]

[a] Laboratório de Ecologia e Conservação Marinha, Instituto do Mar, Universidade Federal de São Paulo, Rua Dr. Carvalho de Mendonça 144, Santos 110-070, Brazil
[b] Geography, College of Life and Environmental Sciences, University of Exeter, Exeter, UK
[c] Instituto de Geociências, Universidade de São Paulo, Rua do Lago 562, São Paulo 05508-080, Brazil
[d] Universidade Federal do Espírito Santo, UFES/Departamento de Oceanografia e Ecologia, Vitória 29075-910, ES, Brazil
[e] Instituto Oceanográfico, Universidade de São Paulo, Praça do Oceanográfico, 191, São Paulo 05508-120, Brazil
[f] Faculty of Geosciences and MARUM-Center for Marine Environmental Sciences, University of Bremen, Leobener Strasse 8, Bremen 28359, Germany
[g] Instituto de Biologia and SAGE-COPPE, Universidade Federal do Rio de Janeiro, Rio de Janeiro, Brazil

ARTICLE INFO

Keywords:
Marginal reefs
Climate change
Subtropical reef
Reef accretion
South Atlantic

ABSTRACT

Whilst the impacts of climatic and oceanographic change on lower latitude reefs are increasingly well documented, our understanding of how reef-building has fluctuated in higher latitude settings remains limited. Here, we explore the timing and longevity of reef-building through the mid- to late Holocene in the most southerly known reef (24°S) in the Western Atlantic. Reef core data show that reef growth was driven by a single coral species, *Madracis decactis*, and occurred over two phases since ~6000 calibrated (cal.) yr B.P.. These records further indicate that there was a clear growth hiatus from ~5500 to 2500 cal. yr B.P., and that there is no evidence of reef accretion on the Queimada Grande Reef (QGR) over the past 2000 yrs. It thus presently exists as a submerged senescent structure colonized largely by non-reef building organisms. Integration of these growth data with those from sites further north (18°S and 21°S) suggests that Intertropical Convergence Zone (ITCZ), South Westerlies Winds (SWW) and El Niño-Southern Oscillation (ENSO) variability and shifts during the Holocene drove changes in the position of the Brazil-Falklands/Malvinas Confluence (BFMC), and that this has had a strong regional influence on the timing and longevity of reef growth. Our results add new evidence to the idea that reef growth in marginal settings can rapidly turn-on or -off according to regional environmental changes, and thus are of relevance for predicting high latitude reef growth potential under climate change.

1. Introduction

Due the additive and interacting forces of global climate changes and local anthropogenic stressors, coral reefs are currently experiencing a collapse without precedent in recent millennia (e.g., Aronson et al., 2002; Aronson et al., 2004; Montaggioni, 2005; Bruno and Valdivia, 2016; Côté et al., 2016). However, we also know that independent of anthropogenic forcing, coral reef health and growth at some sites has fluctuated through the Holocene (e.g., Perry and Smithers, 2011; Toth et al., 2012; Toth et al., 2018; Dechnik et al., 2019; Gischler and Hudson, 2019). Emerging geologic evidence shows the strong influence of regional climatic and oceanographic changes on the timing and longevity of reef development. Two major areas of interest have arisen in recent years in relation to understanding reef growth potential as environmental and ecological conditions change. The first relates to the question of the timescales over which coral reef structures have developed. There is, for example, now evidence from a few select sites that the contemporary coral communities on some reefs are actually ephemeral veneers growing above largely relict physical structures that ceased significant coral reef-building several thousand years before present (e.g., Toth et al., 2018). This has led to debate about the extent to which living coral communities are, or are not, actively contributing to on-

* Corresponding author at: Departamento de Ciências do Mar, Universidade Federal de São Paulo (UNIFESP), R. Dr. Carvalho de Mendonça, 144 Vila Belmiro, Santos, SP 11070-102, Brazil.
E-mail address: pereira.filho@unifesp.br (G.H. Pereira-Filho).

https://doi.org/10.1016/j.gloplacha.2021.103479
Received 17 November 2020; Received in revised form 24 March 2021; Accepted 29 March 2021
Available online 2 April 2021

going reef-building, or how long the ecological function of a coral reef may subsist after its geological senescence (Kuffner and Toth, 2016; Toth et al., 2018; Perry and Alvarez-Filip, 2018).

The second issue concerns how subtle environmental or oceanographic changes may lead to reef growth turn-on or -off (terminology sensu Buddemeier and Hopley, 1988), especially at sites close to the environmental limits of reef development - i.e., in more marginal marine settings (Perry and Larcombe, 2003). In these areas, corals exist close to their environmental thresholds (Kleypas, 1996). Thus, their capacity to build reef structures is likely to be highly dependent on local to regional environmental changes, turning on when favorable or turning off when conditions deteriorate. Examples from the turbid-zone inner-shelf areas of Australia's Great Barrier Reef illustrate how distinct cycles of reef initiation-growth-demise and then, after a hiatus, new reef development have influenced regional patterns of reef development (e.g., Perry and Smithers, 2011). This, in turn, has implications for understanding how reef-building may respond in these more marginal settings under climate change. There has been speculation that the latitudinal range of reef-building corals may expand polewards under ocean warming (e.g., Vergés et al., 2014), and there is evidence from the Pleistocene that this occurred in Western Australia (Greenstein and Pandolfi, 2007). However, our understanding of the timing and sensitivity of reef-building to oceanographic changes within more marginal reef building zones of the global oceans is generally very limited.

Here, we integrate both new and published reef core data to explore the timing and nature of reef-building in the most southerly reef complexes in the Western Atlantic. Specifically, we report age structure data from the Queimada Grande reef (QGR), a high latitude (24°S) subtropical reef located in the Southwestern Atlantic (SWA; Pereira-Filho et al., 2019). We then compare our records of QGR growth with those from the slightly more northerly Abrolhos (18°S) and Anchieta (21°S) reef complexes. Collectively, these data provide an opportunity to explore regional phases of reef growth along this high latitude gradient, and to examine the influence of regional climatic and oceanographic factors on the timing and longevity of reef building over the past ~6000 years.

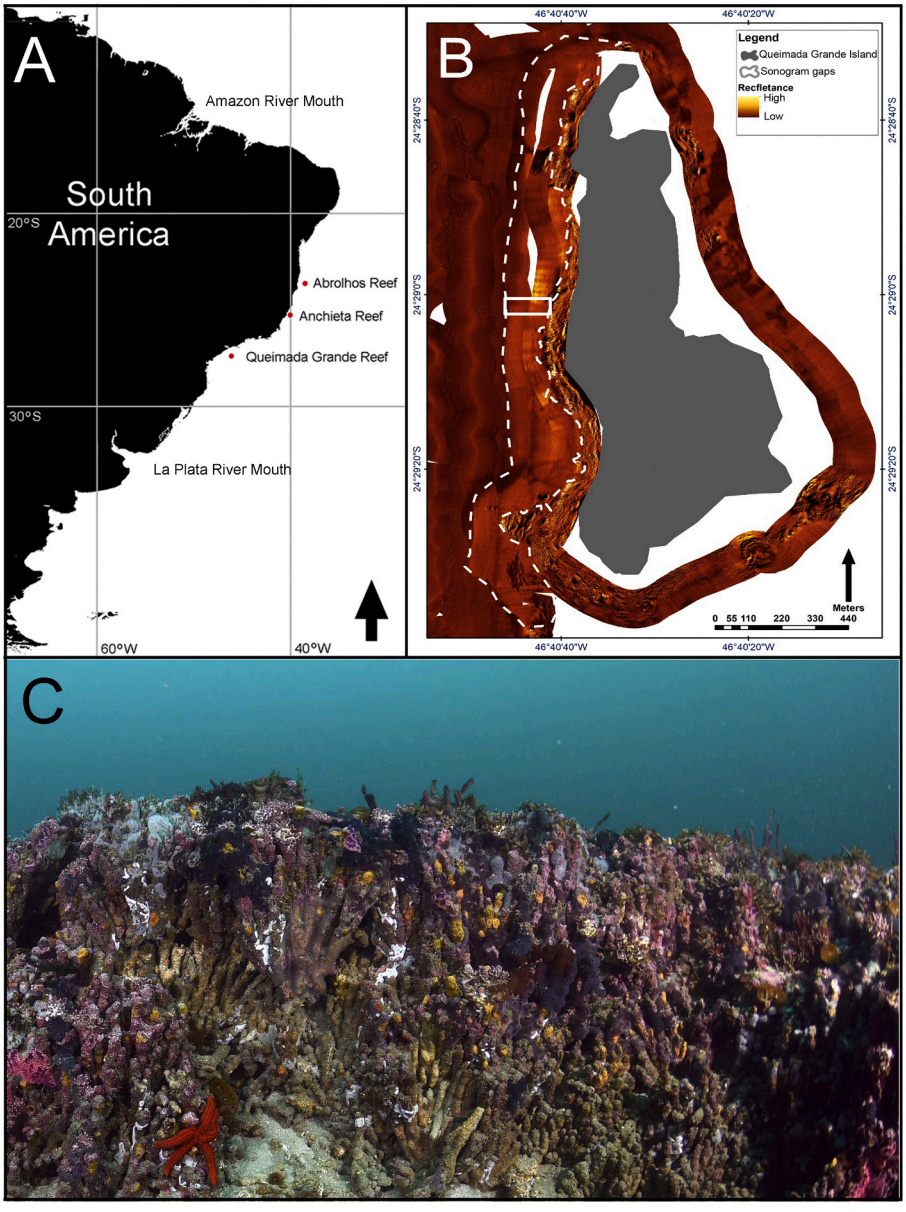

Fig. 1. A) South Atlantic coral reefs for which Holocene reef growth is relatively well know. B) Sonogram of the Queimada Grande Reef (QGR). Hard substrates (i.e., rocky shore and coral reef) are indicated by higher reflectance sign while rhodolith beds (intermediate bottom between hard and soft bottom) are indicated by lower reflectance. White rectangle indicates the coring location, while dashed white line shows the limit of the QGR, with its characteristic reflectance pattern. C) Image illustrating the QGR reef framework build major by *Madracis decactis* encrusted by coralline algae at the top. Space between vertical coral branches is filled with sediments.

2. Methods

2.1. Study area

In the SWA, modern reefs occur from the Amazon river mouth south to 24°S (Moura et al., 2016; Pereira-Filho et al., 2019) and are built by coralline algae, bryozoans and an impoverished coral fauna (~23 coral and 5 hydrocoral species) dominated by massive and encrusting species (e.g. *Mussismilia* spp., *Montastrea cavernosa*, *Siderastrea* spp. and *Madracis decactis*), several of which are endemic (Leão et al., 2016; Pereira-Filho et al., 2019). While coral reefs occur in North Atlantic subtropical areas (e.g., Florida, Bermuda, Bahamas; Toth et al., 2018), only one subtropical coral reef, the Queimada Grande Reef (QGR), is known in the SWA (Fig. 1A). Contrasting with its Atlantic tropical counterparts with their mixed coral, coralline algal and bryozoan frameworks, the QGR framework was built by only one widely distributed coral species, *Madracis decactis* (Pereira-Filho et al., 2019). We also note that whilst the currently depauperate living corals at the site (i.e., only two species *M. decactis* and *Mussismilia hispida*) have a coverage comparable with that another SWA tropical reefs, in the QGR they do not appear to be supporting modern reef accretion/accumulation (Pereira-Filho et al., 2019). The QGR covers ~320,000 m^2 between 10 and 20 m depths (Fig. 1B-C), forming a relatively flat plateau that fringes the subtidal rock shore (~10–20 m depth) on the leeward (western) side of the Queimada Grande Island. The island derives from the regressive erosion of the Serra do Mar scarp which comprises igneous and metamorphic rocks from the Ribeira mobile belt (granite, granulite, migmatite and gneiss) ~750–450 Ma BP (de Almeida et al., 1973). The Queimada Grande Island marine habitats are under a semi-diurnal tidal influence (~1 m of amplitude during spring tidal changes) and are strongly influenced by the South Atlantic Central Water with sea surface temperatures (SST) ranging from 18 to 28 °C (Bio-ORACLE, https://www.bio-oracle.org/). Three morphological palaeo-reef zones can be distinguished across the reef structure. Although depth and in-water conditions made core recovery challenging, short percussion cores were recovered from each "zone" to assess internal reef structure and age. These zones are referred to here for descriptive purposes as: i) proximal reef, ii) mid reef and iii) distal reef. Most coral colonies were preserved in place (i.e., cylindrical dead coral branches vertically disposed and filled by trapped sediment; Fig. 1C).

2.2. Queimada Grande Reef mapping

Side Scan Sonar surveys included contiguous transects parallel to the island's rocky shores between 0 and 40 m depths (Fig. 1B). An Edgetech 4100 system with a 272TD towfish was operated at 100 kHz with 200 and 400 m swaths. Acoustic data were processed using SonarWis Map4 software; geo-referenced mosaics were exported as GeoTiff images with 1 m/pixel resolution into ArcGIS 9.2. Morphological attributes such as area and depth were treated as shapes. The main bottom features identified (i.e., rocky shore, coral reef and rhodolith bed) were confirmed by ~30 h of SCUBA diving deployments.

2.3. Framework description and radiocarbon dating

We obtained three percussion cores with 100% recovery [each ~130 cm - the length of which was limited by safety constraints for emplacing cores in this way in these water depths] along a cross-reef transect that included samples from the proximal reef (14 m water depth), mid reef (13 m) and distal reef (15 m; Fig. 2). Subsamples (n = 15) were collected in a 30-cm-interval from each core, labeled, and treated with HCl to remove superficial contamination.

Radiocarbon dating was performed on coral samples in excellent taphonomic condition (i.e., less than ~20% bioerosion and/or infilling; c.f. Toth et al., 2018). These samples were washed, dried, and reacted under vacuum with 100% phosphoric acid, yielding carbon dioxide, which was cryogenically purified and reduced to graphite (Vogel et al., 1984). Graphite $^{14}C/^{13}C$ ratios were measured using a CAIS 0.5 MeV

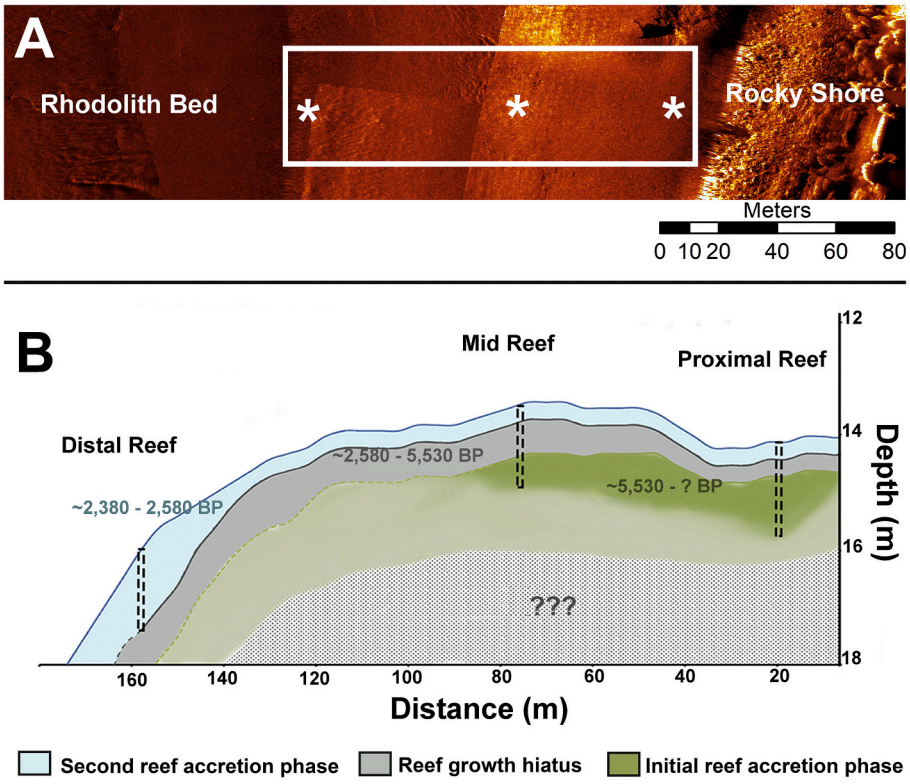

Fig. 2. A) Detailed sonogram where percussion cores were obtained (asterisks). White rectangle corresponds to the same area indicated in Fig. 1B. Rocky shore and rodolith bed were interpreted according their reflectance sign and by ground truth SCUBA diving. B) Schematic cross-section of core locations.

accelerator mass spectrometer (AMS) at the Center for Applied Isotope Studies (University of Georgia). Measured $^{14}C/^{13}C$ ratios were corrected relative to the international reference material NBS SRM 4990 (Oxalic Acid I) and corrected for carbon isotope fractionation based on $\delta^{13}C$ values (expressed in ‰ relative to the V-PDB international reference) measured on separate aliquots using an isotope ratio mass spectrometer (IRMS; analytical precision <0.1‰). Uncalibrated dates are given in radiocarbon years before 1950 (years AD), using the ^{14}C half-life of 5568 years. The error is quoted as two-sigma standard deviation and reflects both statistical and instrumental errors. Calibration of radiocarbon date was performed using the software CALIB Version 8.20 and the calibration curve Marine20 (http://calib.org, accessed 2021-01-10). We used the 10 nearest point ΔR −99 ± 103.0 as the best current estimate of variance in the local open water marine reservoir effect. The median probability age is given as the best estimate of calibrated age. One dating was also obtained from organic matter from sediment. In this case, the calibration curve IntCal20 was applied. Sixty-three radiocarbon dating data from Abrolhos and Anchieta tropical reefs (i.e., 18°S and 21°S, respectively) were compiled from Bastos et al. (2018) and Dechnik et al. (2019).

2.4. Optically stimulated luminescence dating

Luminescence dating was carried out at the Luminescence and Gamma Spectrometry Laboratory (LEGaL) of the Institute of Geosciences of the University of São Paulo. The reef cores were opened under subdued red/amber-light conditions to avoid bleaching of natural luminescence signals, and at least 40 g of sediments were picked from between the coral framework with a small spoon (n = 5). Quartz grains retrieved from these sediment samples were used for optically stimulated luminescence (OSL). Samples were collected at the same depth interval as the ^{14}C dated coral samples and quartz concentrates were prepared following standard procedures as described in Aitken (1998). The 180–250 μm grain size fraction was obtained by wet sieving, followed by chemical treatment with 27% H_2O_2 and 10% HCl to remove organic matter and carbonates, respectively. Subsequently, samples were treated with 48–51% HF for 40 min to remove feldspar and outer rinds of quartz grains dosed by alpha particles. Due to the small amount of sample after the chemical treatment, we decided not to separate quartz from heavy minerals (the absence of feldspar was tested with infrared light), since the signal of heavy minerals are generally one order of magnitude lower than that of quartz (Krbetschek et al., 1997; Del Rio et al., 2019).

The OSL dating method using the single-aliquot regenerative (SAR) dose protocol (Murray and Wintle, 2000; Wintle and Murray, 2006) was carried out on quartz aliquots. Luminescence measurements were performed in a Lexsyg Smart TL/OSL reader equipped with blue and infrared LEDs, filters for light detection in the UV band and beta radiation source ($^{90}Sr/^{90}Y$) with dose rate of 0.116 Gy s^{-1} for steel discs. Dose recovery tests were performed on aliquots bleached for 3 h under a solar simulator lamp. Dose recovery tests were carried out with a preheat temperature of 220 °C and given a dose of 5 Gy. The calculated-to-give dose ratio obtained for the dose recovery test was 0.91. The equivalent dose for each sample was determined by measuring at least 24 quartz aliquots. Exponential fitting of dose-response data was carried out only when the recycling ratio was in the 0.9–1.1 range, and recuperation was <5% and feldspar contamination was negligible. Feldspar contamination in each aliquot was appraised by repeating the first regeneration dose and using infrared stimulation at 60 °C before blue stimulation. Aliquots were rejected when an infrared stimulated luminescence signal was detected, or when the OSL signal was depleted following infrared stimulation. The equivalent dose was determined through the central age model (Galbraith et al., 1999) using at least 13 accepted quartz aliquots per sample.

To calculate dose rates, mean specific activities (Bq kg^{-1}) of ^{238}U, ^{232}Th, and ^{40}K were assessed through gamma ray spectrometry using a high purity germanium (HPGe) detector with energy resolution of 2.1 KeV and relative efficiency of 55%, encased in an ultra-low background shield. Samples were kept in sealed plastic containers for at least 28 days for radon equilibration before gamma ray spectrometry. The conversion factors provided by Guérin et al. (2011) were used for beta and gamma dose rates' calculation. The cosmic dose rate was evaluated using sample depth, altitude, longitude and latitude (Prescott and Stephan, 1982). Moisture content was considered as the maximum water saturation (water weight/dry sample weight) for each sample, by saturating the samples used in dose rate calculation. The OSL ages were calculated by dividing the equivalent dose value by the dose rate value (Table 1).

2.5. Sediment analysis

In the three reef cores, sediment samples (n = 72) were collected manually in a 4 cm vertical spacing, using a small spoon. Only sediment trapped in the reef framework among coral colonies (10–15 ml) was sampled. All samples were wet sieved in a 0.5 mm mesh to remove larger coral fragments resulting from core processing. After sieving, samples were oven-dried, weighted and treated with HCl and H_2O_2 to remove carbonates ($CaCO_3$) and organic matter (OM), respectively. Samples were washed with distilled water, dried and weighed after chemical treatment in order to calculate carbonate and OM contents. Grain-size analyses were performed for all samples, after chemical treatment, using a Malvern Mastersizer 2000 laser granulometer coupled with a Hydro 2000MU dispersion unit (distilled water used as dispersion medium) and a built-in ultrasound device. Descriptive statistics parameters were calculated according Pearson's moments method. Size fractions are given in 0.125 phi interval (Wentworth, 1922). Since silt and fine sand were the dominant size fractions in all samples, the ratio (silt + fine sand)/silt was calculated in order to evaluate the variation of these fractions without auto correlation.

3. Results

Side scan sonar mapping revealed that the major bottom features of the QGR can be delineated into three palaeo reef zones on the basis of their morphology, relative depth and position relative to the shoreline: an distal reef zone (distal from the rock shore) with an inclination of ~30° at the deepest portion (between depths of 15 to 25 m relative to present MSL); an proximal reef zone, located close to the shore at a depth of ~14 m; and between these an mid reef zone, at a depth of ~13 m (Fig. 2). Radiocarbon dating of coral clasts in cores also clearly demonstrates that the present reef surface is essentially a relict feature, and that whilst the cores did not capture the reef initiation phase, it is clear that the reef was actively accreting prior to 6000 cal. yr. B.P.. Analysis of cores from each of these palaeo reef zones indicates: i) that the QGR is constructed entirely of one cylindrical branched coral species *Madracis decactis*; and ii) that the accumulating reef framework comprises intermixed units of in-place and detrital coral rubble, with non-reefal units between (defined by the lack of any coral material; Fig. 3).

Cores from the interpreted proximal and mid reef zones identify two apparently distinct phases of reef growth since ~6000 cal. yr. B.P.. These occurred between 5749 and 5677 cal. yr. B.P. and between 2380 and 2586 cal. yr. B.P., with a non-depositional hiatus in between (median probability ages are presented as the best estimate of ^{14}C calibrated ages, the complete data are available in Table 2 and Fig. 3). In the proximal reef core, dates ranged between 5749 (base of core) to 2533 cal. yr. B.P. (top of core), but with no evidence of framework accumulation between ~5677 and 2501 cal. yr. B.P.. This period of time is represented by a time condensed sediment interval ~ 15 cm thick devoid of coral material (Fig. 3). Sediments recovered along the core (i.e., among coral branches and deposited during the reef hiatus interval) are composed mostly of carbonates whose abundance ranged between 55% and 75%, organic matter content varied from 1% to 5%, with one peak coinciding with lower carbonate contents at ~60 cm (Fig. 4). While

Table 1
Optically stimulated luminescence age analysis. PR – Proximal Reef, MR – Mid Reef, and DR – Distal Reef.

Sample (Core depth)	Accepted aliquots	Equivalent dose (Gy)	Overdispersion (%)	K (%)	^{238}U (ppm)	^{232}Th (ppm)	Cosmic dose rate (Gy. ky-1)	Total dose rate	Age (years)
PR(60 cm)	19/25	1.78	24.4	0.31	0.618	3.463	0.0744	0.494	3602 ± 388
MR(60 cm)	13/15	1.54	18	0.40	0.594	2.497	0.0744	0.525	2931 ± 229
DR (30 cm)	3/5	1.28	27.2	0.50	0.54	2.230	0.0744	0.518	2472 ± 514
DR (60 cm)	20/26	1.59	9	0.72	1.043	2.526	0.0744	0.726	2189 ± 185
DR (90 cm)	11/12	1.54	13.5	0.50	0.61	1.970	0.0744	0.576	2674 ± 229

organic matter recovered from 56 cm returned a ^{14}C age of 4730 cal. yr. B.P. (with a δ^{13}C value of −24.14‰ suggesting a continental origin from C3 plants), quartz OSL ages from the same portion indicate that sedimentation occurred around 3602 ± 388 years ago [i.e., optically stimulated luminescence (OSL) age analysis, see Fig. 4 and Tables 1 and 2]. This ~1000 years lag between terrestrial carbon fixation and sediment deposition suggests distant sources of fine sediment portions deposited ~3600 years ago.

In the "mid reef" core, dates ranged between 5556 (base of core) and 2489 cal. yr. B.P. (at core top; Table 2). No in place coral occurred in the core between a depth of ~40–80 cm, and this depositional interval also indicates a period lacking reef framework accumulation between ~5500 and ~2500 cal. yr. B.P. (Fig. 3). The only ^{14}C datable carbonate in this non-reefal unit were serpulids tubes (i.e., sessile polychaete) which returned an age of ~3300 cal. yr. B.P.. Sediments were composed mostly of carbonates that ranged between 50% and 80%. Organic matter content varied from 1% to 8%, higher percentages coinciding with lower carbonate contents at 40 cm (Fig. 4). Sediments from the non-reefal unit, where serpulids were found, returned a broadly comparable OSL age of 2931 ± 229 years ago (Figs. 3 and 4 and Table 1) and suggests higher rates of sedimentation during periods unfavorable to the coral growth.

The distal reef core was collected at 15 m depth. It similarly contained in place coral skeletons all of which dated to the post-hiatus period identified in the mid and proximal reef cores above (dates ranged from 2366 and 2478 cal. yr. B.P.). Although some age inversions could be suggested by calibrated ages, they are not significant considering the error bars of radiocarbon dating and may be indicative of a mix of both in place but also some transported (from shallower zone) coral clasts. In this reef zone (i.e., the distal reef), where 1 m of the core comprises approximately 100 years of deposition, three distinct sedimentary horizons are discernible characterised by an increase in sand and a decrease in silt contents, and may indicate a period of depositional interruption, or again event horizons (Figs. 3 and 4). Sediments seem to be have trapped soon after reef framework accumulation based on difference between coral growth (i.e., C14) and sedimentation (i.e., OSL; Tables 1 and 2). Carbonate content is in the range of 45%–60%, while organic matter content varied from 2.5% to 15%, with higher concentration coinciding with lower carbonate contents (Fig. 4).

4. Discussion

Core records from the sub-tropical QGR show clear evidence for a Mid-Holocene cessation in framework accumulation at this site. Although we could not determine when reef growth initiated at these sites, our data indicate that the reef was clearly accreting prior to 6000 cal. yr. B.P. when the regional sea level was in a late stages of rise before reaching a highstand at ~5500 cal. yr. B.P. (~4 m above the present; Angulo et al., 1999, 2006; Angulo et al., 2013; Toniolo et al., 2020; Fig. 5). Nevertheless, the current depth of the palaeo-reef surface and coral ages from its surface indicate that the QGR never reached sea level (Fig. 5). Thus, regional sea-level rise (SLR) was not the major driver of vertical growth in terms of providing space for reef accommodation such as has been reported for reefs northward from QGR (i.e., Anchieta and Abrolhos reefs; 20°S and 18°S, respectively; Dechnik et al., 2019, Vasconcelos et al., 2018; Fig. 5) and many other tropical reefs. Furthermore, the relatively limited amount of RSL rise that occurred over the period of interest here argues against sudden jumps in sea level leading to either reef drowning or back-stepping (sensu Blanchon et al., 2002). Instead, our data add evidence to support the idea that reef-building in marginal settings is strongly influenced by regional climatic and oceanographic changes. These changes impact both the timing and longevity of reef development, with reefs turning on or turning off when conditions are favorable or unfavorable. In the QGR records our data suggest four episodes of reef development and demise: i) an initial reef accretion phase (RAP) up to ~5500 cal. yr. B.P.; ii) a hiatus phase between ~5500 and ~ 2500 cal. yr. B.P.; iii) a second phase of reef framework accumulation at ~2600 to ~2400 cal. yr. B.P.; and, iv) the post ~2300 y B.P. period during which no further reef accretion occurred. Interestingly, the Mid to Late Holocene reef growth phases described here have also been reported for other regions such as the Southern Pacific (Woodroffe et al., 2010; Perry and Smithers, 2011), the Northwestern Pacific (Hamanaka et al., 2012), the western coast of Panama (Toth et al., 2012), and the tropical southwestern Atlantic (Dechnik et al., 2019).

SLR has previously been evoked as having influence on Mid to Late Holocene reef growth in SWA tropical areas (e.g., at Anchieta Reef and Abrolhos Reef, 20°S and 18°S, respectively). However, this period was also accompanied by other climatic and oceanographic changes that may explain changes in reef accretion phases in high latitude settings such as the Queimada Grande subtropical reef. For instance, RAP I may relate to a southward displacement of the Inter-Tropical Convergence Zone (ITCZ), coupled with Southern Westerly Wind (SWW) weakening (Mariani et al., 2017), changes which have been attributed to the movement of the South Atlantic Subtropical Dipole (SASD; Wainer et al., 2014). Specifically, shifts in the SWW are known to have altered the position of the Brazil-Falklands/Malvinas Confluence (BFMC) during the Holocene (Voigt et al., 2015). The BFMC is one of the world's most energetic oceanographic features and a major driver of freshwater, sediment and nutrient dispersion from the La Plata River (Peterson and Stramma, 1991; Brandini et al., 2000; Gu et al., 2019). Currently, the south-flowing Brazil Current (BC) converges with the north-flowing Falklands/Malvinas Current (FMC) at ~38°S, and the La Plata discharge influence reaches ~25°S (Gyllencreutz et al., 2010; Fig. 6A). From 8700 to 5500 cal. yr. B.P., as a consequence of SWW weakening, the BFMC shifted from its Mid Holocene northernmost position (Fig. 6B) southward, resulting in warmer SSTs at 24°S (Voigt et al., 2015; Gu et al., 2019). These relatively warm conditions, combined with lower El Niño-Southern Oscillation (ENSO) frequencies, prevailed until ~5500 cal. yr. B.P. (Hodell and Kanfoush, 2001; Voigt et al., 2015; Gu et al., 2019), conditions that we suggest favoured reef development at QGR and probably also influenced other Southwestern Atlantic tropical reefs (Dechnik et al., 2019; Fig. 6C). Wider evidence for this warmer South Atlantic SST period occur in cores from 53°S, which exhibit foraminifera

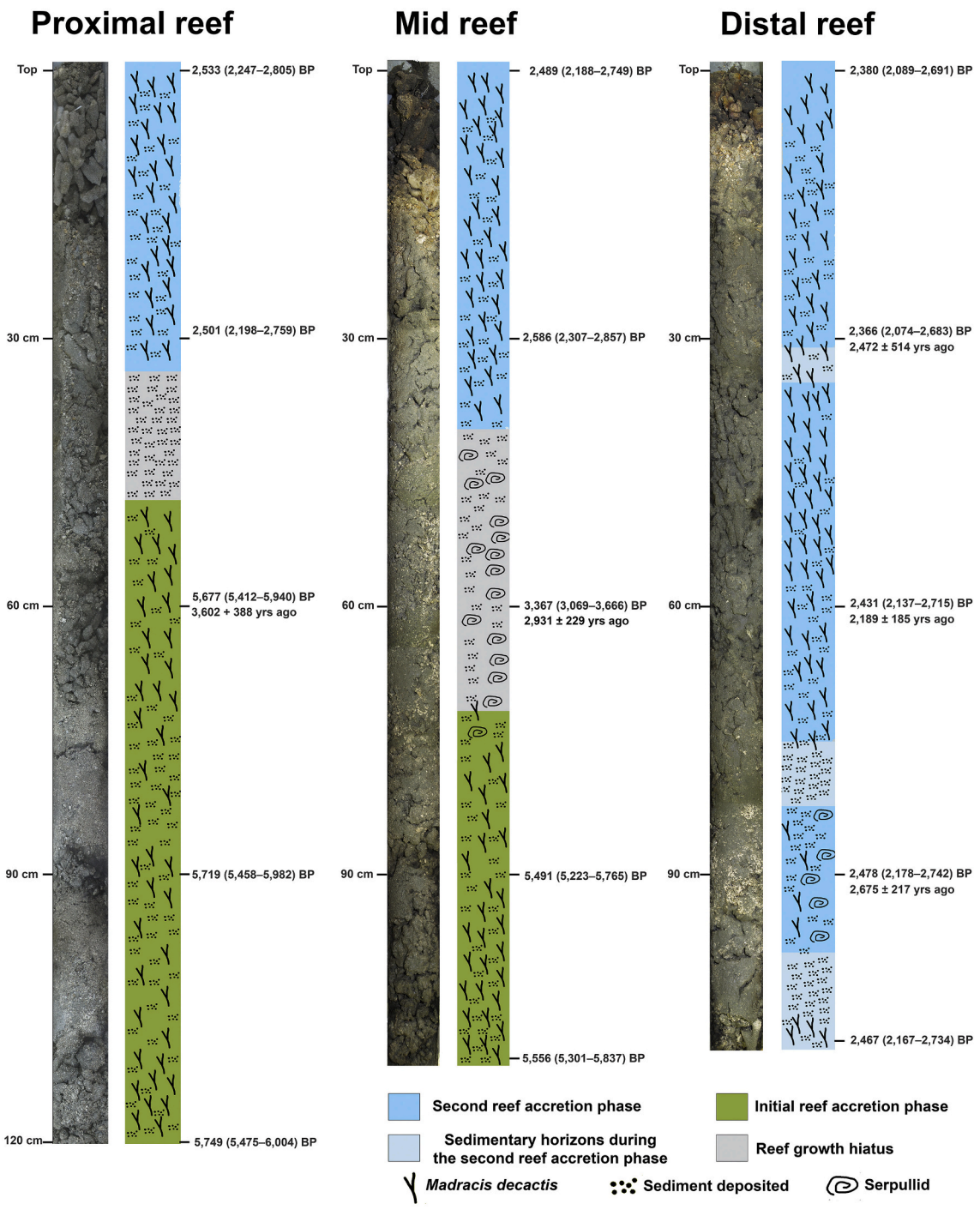

Fig. 3. Stratigraphic position and calibrated AMS radiocarbon ages [years Before Present (B.P.)] of the coral samples (excepted at 60 cm mid reef where serpulid worm tube was dated) and OSL ages of sediment (years ago). Vertical axis indicates the core depth.

abundance peaks up to 6500 cal yr. B.P. (Fig. 6D). This warm period was also marked by latitudinal expansion of Pacific South America lowland thermophilous trees (Moreno, 2004).

The QGR then "turned off" from ~5500 through to ~2500 cal. yr. B.P., a change we interpret as a function of deteriorating (for coral growth) oceanographic conditions in this marginal marine setting. Evidence from elsewhere in the Southern Ocean would suggest that this is likely to have been driven by significant SST cooling and ice expansion further south (Fig. 6E). Specifically, during this period, there is evidence for an apparent decoupling of the ITCZ and SWW, as a consequence of AMOC stability (Mariani et al., 2017). This resulted in the northward migration of Antarctic winter sea ice as a consequence of weakened polar maritime air masses (Hodell and Kanfoush, 2001), and an increasing importance of ENSO (El Niño and La Niña) in modulating climate (Toth et al., 2012; Mariani et al., 2017). Terrestrial records from this time also show vegetation being replaced by cold-resistant rain forest trees (Moreno, 2004). Negative SASD records (Wainer et al., 2014), absence of foraminifera up to ~1830 cal. yr. B.P. in cores from 53°S (Hodell and Kanfoush, 2001; Fig. 6D-F) and Sr/Ca records on vermitid shells from 23°S to 26°S (Toniolo et al., 2020) corroborate this interpretation. Interestingly, a similar period of reef growth hiatus in the Northwestern Pacific (i.e., ~29°N) is also explained by cold SSTs as consequences of

Table 2
Radiocarbon ages and $\delta^{13}C$ and $\delta^{18}O$ values and Optically Stimulated Luminescence dating parameters. Calibration of radiocarbon datings was performed using the software CALIB Version 8.20 and the Marine20 calibration curve (http://calib.org). We used the ten nearest points ΔR −99 ± 103.0 as the best estimate of the local open water marine reservoir effect and referring to 2 sigma calibrated range. The median probability age is given as the best estimate of calibrated age.

Radiocarbon ages								
Core	Lab Code	Material	Core depth (cm)	$\delta^{13}C$‰	$\delta^{18}O$‰	^{14}C years BP	Years Cal BP	Median probability
Proximal Reef	UGAMS35182	Coral	Top	−1.23	−2.15	2840 (±20)	2247–2805	2533
	UGAMS35183	Coral	30	−1.40	−1.75	2810 (±20)	2198–2759	2501
	UGAMS35184	Coral	60	−1.27	−1.49	5390 (±25)	5412–5940	5677
	UGAMS 39087[a]	Sediment	60	−24.14	–	4210 (±25)	4576–4859	4730[a]
	UGAMS 35185	Coral	90	−1.45	−2.10	5430 (±25)	5458–5982	5719
	UGAMS 35186	Coral	120	−1.22	−1.74	5460 (±20)	5475–6004	5749
Mid Reef	UGAMS 35177	Coral	Top	−1.12	−1.60	2800 (±20)	2188–2749	2489
	UGAMS35178	Coral	30	−1.34	−1.96	2890 (±20)	2307–2857	2586
	UGAMS35179[b]	Serpullid	60	2,09	0.15	3530 (±20)	3069–3666	3367[b]
	UGAMS35180	Coral	90	−1.51	−1.56	5220 (±20)	5223–5765	5491
	UGAMS 35181	Coral	100	−1.18	−1.67	5280 (±20)	5301–5837	5556
Distal Reef	UGAMS35187	Coral	Top	−2.26	−1.30	2710 (±20)	2089–2691	2380
	UGAMS35188	Coral	30	−1.19	−1.85	2700 (±20)	2074–2683	2366
	UGAMS35189	Coral	60	−1.79	−1.40	2750 (±20)	2137–2715	2431
	UGAMS35190	Coral	90	−1.00	−1.27	2790 (±20)	2178–2742	2478
	UGAMS35191	Coral	100	−1.73	−1.76	2780 (±20)	2167–2734	2467

[a] Organic matter from sediment (in this case the IntCal20 calibration curve was used).
[b] Non-coral sample (i.e., Serpulid tubes).

changes in oceanographic regional patterns (i.e., a Kuroshio Current weakening; Hamanaka et al., 2012). Sediment coarsening (higher contributions of sand) coincides with peaks in the carbonate fraction in the QGR, suggesting an increase in wave/current energy during the hiatus (Fig. 3). While increases in the carbonate fraction seem related to reef erosion, terrigenous sand increases are likely associated with remobilization of sediments from the inner shelf by offshore transport. Indeed, the reef growth hiatus at QGR is concurrent with the lowest rates of sediment retention by a coastal sand barrier located in its nearest estuarine system (Guedes et al., 2011). Additionally, differences between sediment depositional ages (OSL dated at 3602 years ago) and organic matter radiocarbon ages (4741 cal. yr. B.P.) during the reef growth hiatus period suggest distant sources for the fine organic sediments. Indeed, values of δ13C (i.e., −24 to −23‰, see Table 2) indicates C3 continental plants (Meyers, 2003) that would be consistent with influence of the South America drainage system during the Mid to Late-Holocene, including Plata River plume.

The second short phase of reef growth at QGR (RAP II) occurred from ~2500 to 2300 cal. yr. B.P.. Relative sea level fell ~4 m around this time towards present levels (Fig. 4), probably elevating light penetration on the submergent reef surface. However, waning La Niña and reduced El Niño strength linked with weakened SWW, as well as a positive SSAD, were likely key drivers of this period of renewed reef growth, which is also evident in Abrolhos reef (18°S; Fig. 6C and F-G). Reduced terrigenous sediment content in cores also suggests a reduction in wave/current energy at QGR around ~2500 years B.P. (Fig. 4). However, the synergistic effects of these conditions, which were favorable to coral growth, lasted a very short time (~200–300 years) and were followed by a period with the highest ENSO variability recorded during the Holocene (i.e., since ~2000 cal. yr. B.P.; Fig. 6G). While SSE winds during La Niña would have increased the northward penetration of the La Plata plume and colder conditions, El Niño is linked to higher precipitation around 24°S. This shift in ENSO frequency corresponds to a coarsening of the sand fraction in the cores (Fig. 4). Late Holocene reef turn-on has also been reported in other areas that are directly affected by ENSO (i.e., the southwestern and northeastern Pacific), although at these locations reef accretion has generally persisted until present.

Since ~2000 cal. yr. B.P., the QGR has thus existed in an essentially senescent state as a submerged structure colonized by non-reef building organisms. These include fleshy and turf algae, the soft coral *Palythoa caribaeorum*, sponges (e.g., *Aplysina fulva*, *A. caissara*, and *Scopalina ruetzleri*), tunicates, and colonies of the hermatypic corals *Mussismilia hispida*, *Madracis decactis* and crustose coralline algae (Pereira-Filho et al., 2019), although the latter are not sufficiently abundant to add framework to the structure. *M. hispida*, which is the most common coral of these contemporary reefs (i.e., ~15% of benthic coverage) was not recovered in our cores. This may reflect later colonization by *M. hispida*, which is at its very southern limits of occurrence (also corroborated by recent molecular data, Peluso et al., 2018). In contrast, the only coral recovered in cores - i.e., *Madracis decactis* - is widely distributed throughout the Atlantic Ocean (from ~32°N to ~27°S down to 30 m depth). It is thus readily acclimated to suboptimal conditions and capable of exploiting favorable environmental shifts at its limits of occurrence (i.e., subtropical regions) to sustain localised reef development.

Similar reef-building phase-shifts also occurred in the SWA's largest and most speciose reefs (i.e., Abrolhos Reefs, 17–19.5° S). At this more northerly location (~1000 km north of QGR) corals were also the major framework builders up to ~2000 cal. yr. B.P. (Bastos et al., 2018). However, in contrast to QGR, reef growth has continued at Abrolhos over the last ~2000 years, although it has not been driven by corals but by bryozoans. The absence of on-going reef accretion at QGR thus probably reflects its reliance on sufficient densities of the sole Holocene reef-builder *M. decactis* to drive framework accumulation. We also noted that the Holocene sequences reported here are thinner than those reported in other South Atlantic tropical reefs (e.g., Vasconcelos et al., 2018; Bastos et al., 2018; Dechnik et al., 2019), which would be expected given the very southerly location of the QGR (i.e., 24°S). The lack of contemporary reef-building at this site, combined with the evidence of past reef growth phases, illustrates how even subtle shifts in climatic and oceanographic conditions in such marginal settings can rapidly turn-on or -off reef growth, an observation of relevance for predicting high latitude reef growth potential under climate change.

5. Conclusion

Our data show that SWA reefs growth has experienced distinct phases of turn-on and -off throughout the Mid- to Late-Holocene period. Beyond the well know influence of SLR on reef growth, our data suggest a strong influence of regional climate changes in driving SWA reef development over the last ~6000 yrs. B.P.. Thus, this study contributes to a broader understanding of marginal reefs by adding new evidence to the idea that reef growth potential in these marine settings can rapidly change according to environmental changes. Clearly, the logistical

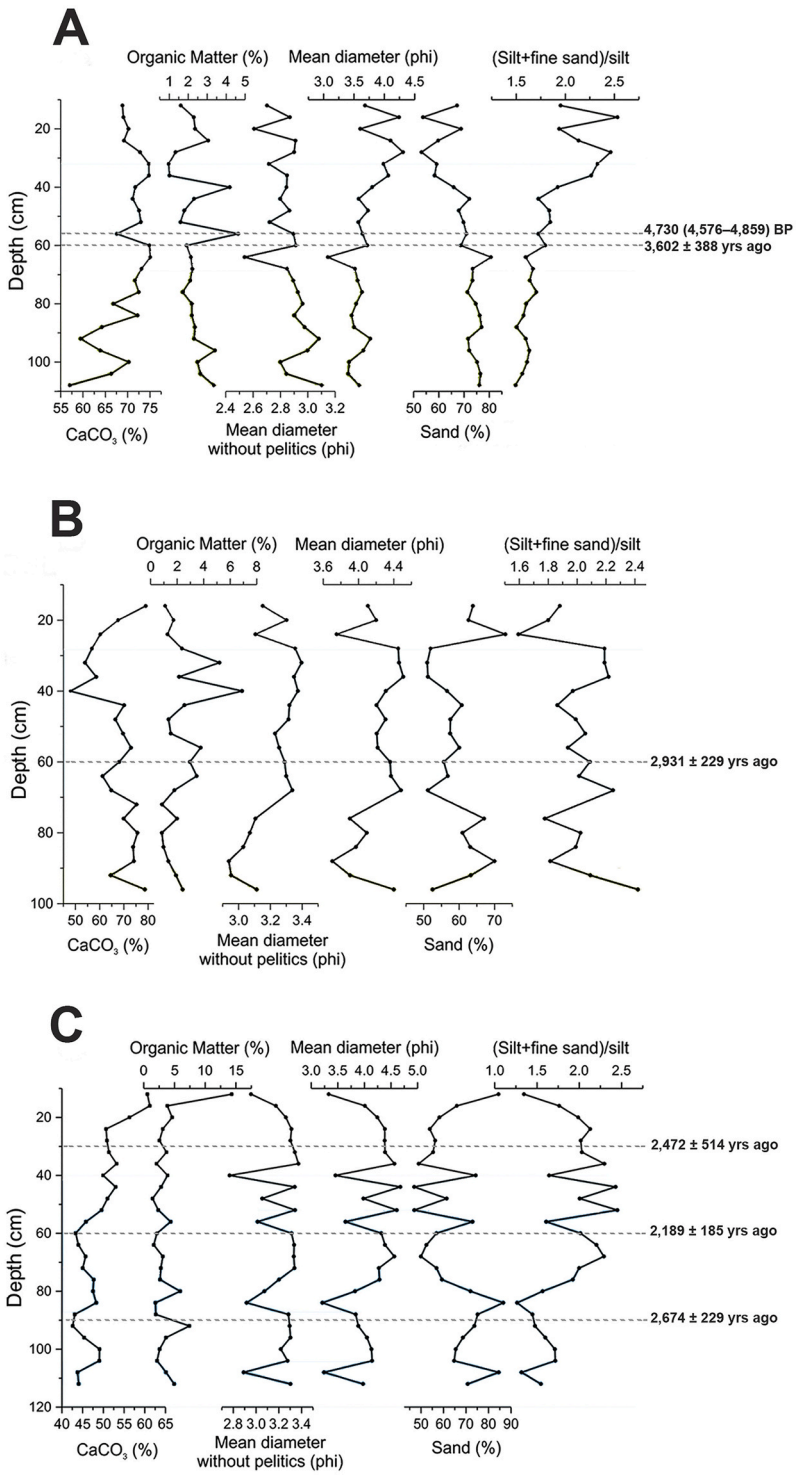

Fig. 4. Vertical profiles of $CaCO_3$, organic matter content (%) and grain size parameters. Horizontal dashed lines indicate sediment OSL age (years ago) or radiocarbon age from organic matter content (cal years B.P.). A) Proximal Reef, B) Mid Reef and C) Distal Reef.

issues that prevented longer and more extensive core recovery necessitate some caveats on our interpretation, however the consistency with the timing of reef growth transitions in slightly more northerly reefs in this region, provide support to the patterns we identify. More widely it is important to emphasise that knowledge on high latitude reef development generally, but of South Atlantic reef development specifically, remains limited and important questions are still unanswered. For instance, there has been recent debate regarding the resilience of the SWA reef-building corals, with some evidence indicating high susceptibility to global warming (Duarte et al., 2020), but other evidence suggesting that corals in SWA marginal marine settings may be highly resilient when facing this modern challenge (Mies et al., 2020). Here, we add geological pieces to this intricate puzzle by showing that SWA reefs alternated between reef development and demise throughout the last ~6000 years.

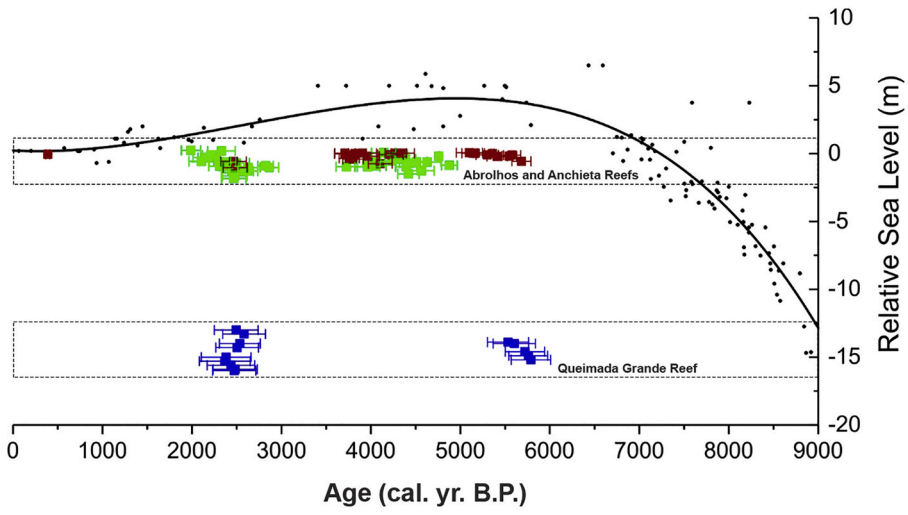

Fig. 5. Holocene Relative Sea Level curve for the Southwestern Atlantic after Angulo et al. (1999, 2006, 2013)) and Toniolo et al., 2020. Reef growth phases are represented according to calibrated radiocarbon datings of corals from Anchieta (green), Abrolhos (brown) and Queimada Grande Reef (blue; 18°S, 21°S and 24°S, respectively). Error bars correspond to two-sigma standard deviation from the mean of the probability distribution of radiocarbon ages, and reflects both statistical and instrumental uncertainties. (For interpretation of the references to colour in this figure legend, the reader is referred to the web version of this article.)

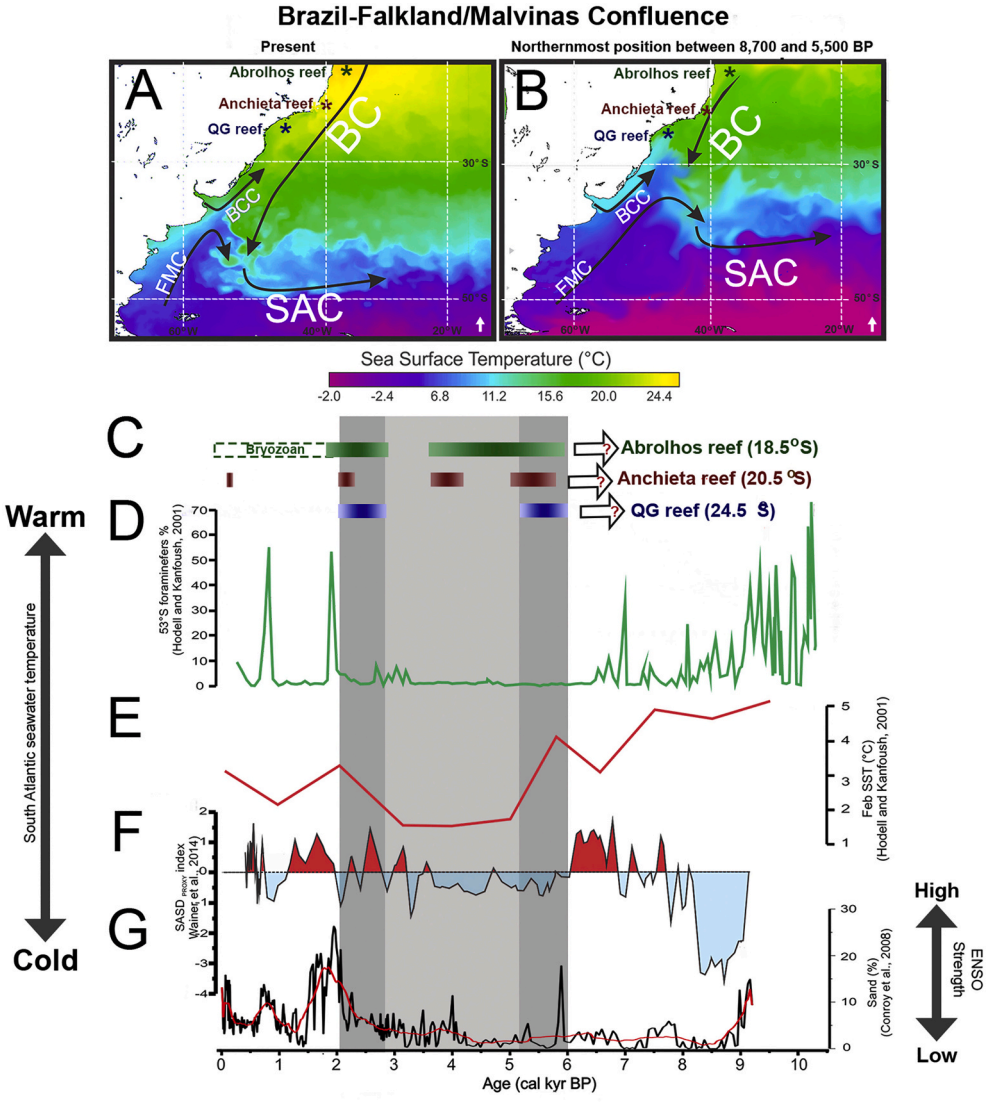

Fig. 6. A) Schematic position of the Brazilian Falkland/Malvinas Confluence (BFMC) and the major oceanographic features; i.e., South Atlantic Current (SAC), Falkland/Malvinas Current (FMC), Brazilian Current (BC) and Brazilian countercurrent (BCC). Sea surface temperature data correspond to February 1998 (obtained from NOAA products website, https://www.ospo.noaa.gov/data/sst/mean_mon/February.98.monmean.gif). B) BFMC northernmost position between 8700 and 5500 BP, based on Gu et al. (2019). Temperature information is merely schematic and was produced hypothesizing the northward displacement of the current fronts presented in A in order to illustrate our hypothesis. C) Rapid accretion phases of the Southwestern Atlantic reefs (i.e., Abrolhos, Anchieta and Queimada Grande Reefs; i.e., calibrated median probability and two-sigma standard deviation), shaded vertical grey bars indicate reef accretion phases and hiatus (dark and ligh, respectively) D) Foraminifera abundance (%; 53°S) from Hodell and Kanfoush (2001). E) February sea surface temperature estimated from diatom assemblages from Hodell and Kanfoush (2001). F) South Atlantic Subtropical Dipole index during the Holocene from Wainer et al. (2014). G) El Niño Southern Oscillation (ENSO) reconstructions from El Junco Lake (Conroy et al., 2008).

Declaration of Competing Interest

The authors declare that they have no known competing financial interests or personal relationships that could have appeared to influence the work reported in this paper.

Acknowledgements

We thank two anonymous reviewers for their detailed, helpful and supportive comments on the manuscript. We thank the Instituto Chico Mendes de Conservação da Biodiversidade (ICMBio) and the staff of Estação Ecológica Tupiniquins and Área de Relevante Interesse Ecológico Ilhas da Queimada Pequena e Queimada Grande for survey permits (SISBIO/62883-2). D. Ricardo for field sampling support. GH Pereira-Filho acknowledges financial support from Fundação de Amparo à Pesquisa do Estado de São Paulo (FAPESP; proc. 2016/14017-0). Finally, we acknowledge individual grants from the Brazilian Research Council (CNPq; GH Pereira-Filho, AO Sawakuchi, AC Bastos, RL Moura and PCF Giannini).

References

Aitken, M.J., 1998. An Introduction to Optical Dating. Oxford University Press, New York.

de Almeida, F.F.M., Amaml, G., Cordani, U.G., Kawashita, K., 1973. The Precambrian evolution of the South American cratonic margin south of the Amazon River. In: Nairn, A.E.M., Stehli, F.G. (Eds.), The Ocean Basin and Margins, 1. Plenum Press, New York, N.Y., pp. 441–446

Angulo, R.J., Giannini, P.C., Suguio, K., Pessenda, L.C., 1999. Relative sea-level changesin the last 5500 years in southern Brazil (Laguna e Imbituba region, Santa Catarina State) based on vermetid 14C ages. Mar. Geol. 159 (1e4), 323–339.

Angulo, R.J., Lessa, G.C., Souza, M.C., 2006. A critical review of mid- to late-Holocene Sea-level fluctuations on the eastern Brazilian coastline. Quat. Sci. Rev. 25 (5–6), 486–506. https://doi.org/10.1016/j.quascirev.2005.03.008.

Angulo, R.J., Souza, M.C., Fernandes, L.A., Disaró, S.T., 2013. Quaternary Sea-level changes and aeolianites in the Fernando de Noronha archipelago, northeastern Brazil. Quat. Int. 305, 15–30. https://doi.org/10.1016/j.quaint.2012.12.029.

Aronson, R.B., Macintyre, I.G., Precht, W.E., Murdoch, T.J.T., Wapnick, C.M., 2002. The expanding scale of species turnover events on coral reefs in Belize. Ecol. Monogr. 72, 150–166. https://doi.org/10.2307/3100026.

Aronson, R.B., Macintyre, I.G., Wapnick, C.M., O'Neill, M.W., 2004. Phase shifts, alternative states, and the unprecedented convergence of two reef systems. Ecology 85, 1876–1891. https://doi.org/10.1890/03-0108.

Bastos, A.C., Moura, R.L., Moraes, F.C., Vieira, L.S., Braga, J.C., Ramalho, L.V., Amado-Filho, G.M., Magdalena, U., Webster, J.M., 2018. Bryozoans are major modern builders of South Atlantic oddly shaped reefs. Sci. Rep. 8, 9638. https://doi.org/10.1038/s41598-018-27961-6.

Blanchon, P., Jones, B., Ford, D.C., 2002. Discovery of a submerged relic reef and shoreline off Grand Cayman: further support for an early Holocene jump in sea level. Sediment. Geol. 147 (3–4), 253–270. https://doi.org/10.1016/S0037-0738(01)00143-9.

Brandini, F.P., Boltovskoy, D., Piola, A., Kocmur, S., Röttgers, R., Abreu, P.C., Lopes, R. M., 2000. Multiannual trends in fronts and distribution nutrients and chlorophyll in the southwestern Atlantic (30-62°S). Deep-Sea Res. 147 (1015–1033) https://doi.org/10.1016/S0967-0637(99)00075-8.

Bruno, J.F., Valdivia, A., 2016. Coral reef degradation is not correlated with local human population density. Sci. Rep. 6, 29778. https://doi.org/10.1038/srep29778.

Buddemeier, R.W., Hopley, D., 1988. Turn-ons and turn-offs: Causes and mechanisms of the initiation and termination of coral reef growth. In: Proceedings 6th International Coral Reef Symposium, Australia, vol. 1, pp. 253–261.

Conroy, J.L., Overpeck, J.T., Cole, J.E., Shanahan, T.M., Steinitz-Kannan, M., 2008. Holocene changes in eastern tropical Pacific climate inferred from a Galapagos lake sediment record. Quat. Sci. Rev. 27 (11–12), 1166–1180. https://doi.org/10.1016/j.quascirev.2008.02.015.

Côté, I.M., Darling, E.S., Brown, C.J., 2016. Interactions among ecosystem stressors and their importance in conservation. Proc. Biol. Sci. 283, 1–9. https://doi.org/10.1098/rspb.2015.2592.

Dechnik, B., Bastos, A.C., Vieira, L.S., Webster, J.M., Fallon, S., Yokoyama, Y., Nothdurft, L., Sanborn, K., Batista, J., Moura, R., Amado-Filho, G., 2019. Holocene reef growth in the tropical southwestern Atlantic: evidence for sea level and climate instability. Quat. Sci. Rev. 218, 365–377. https://doi.org/10.1016/j.quascirev.2019.06.039.

Del Rio, I., Sawakuchi, A.O., Giordano, D., Mineli, T.D., Nogueira, L., Abele, T., Atencio, D., 2019. Athermal stability, bleaching behavior and dose response of luminescence signals from almandine and kyanite. Ancient TL 37, 11–21.

Duarte, G.A.S., Villela, H.D.M., Deocleciano, M., Silva, D., Barno, A., Cardoso, P.M., Vilela, C.L.S., Rosado, P., Messias, C.S.M.A., Chacon, M.A., Santoro, E.P., Olmedo, D. B., Szpilman, M., Rocha, L.A., Sweet, M., Peixoto, R.S., 2020. Heat waves are a major threat to turbid coral reefs in Brazil. Front. Mar. Sci. 7, 179. https://doi.org/10.3389/fmars.2020.00179.

Galbraith, R.F., Roberts, R.G., Laslett, G.M., Yoshida, H., Olley, J.M., 1999. Optical dating of single and multiple grains of quartz from Jinmium rock shelter, northern Australia: part I, experimental design and statistical models. Archeometry 41 (2), 339–364. https://doi.org/10.1111/j.1475-4754.1999.tb00987.x.

Gischler, E., Hudson, J.H., 2019. Holocene tropical reef accretion and lagoon sedimentation: a quantitative approach to the influence of sea-level rise, climate, and subsidence (Belize, Maldives, French Polynesia). Depos. Rec. 5 (3), 515–539. https://doi.org/10.1002/dep2.62.

Greenstein, B.J., Pandolfi, J.M., 2007. Escaping the Heat: Range Shifts of Reef Coral Taxa in Coastal Western Australia: Global Change Biology, vol. 14, pp. 513–528. https://doi.org/10.1111/j.1365-2486.2007.01506.x.

Gu, F., Chiessi, C.M., Zonneveld, K.A.F., Behling, H., 2019. Shifts of the Brazil-Falklands/Malvinas Confluence in the western South Atlantic during the latest Pleistocene–Holocene inferred from dinoflagellate cysts. Palynology 43 (3), 483–493. https://doi.org/10.1080/01916122.2018.1470116.

Guedes, C.C.F., Giannini, P.C.F., Sawakuchi, A.O., DeWitt, R., Nascimento Jr., D.R., Aguiar, V.A.P., Rossi, M.G., 2011. Determination of controls on Holocene barrier progradation through application of OSL dating: the Ilha Comprida Barrier example, Southeastern Brazil. Mar. Geol. 285, 1–16. https://doi.org/10.1016/j.margeo.2011.04.005.

Guérin, G., Mercier, N., Adamiec, G., 2011. Dose-rate conversion factors: update. Ancient TL 29 (1), 5–8.

Gyllencreutz, R., Mahiques, M.M., Alves, D.V.P., Wainer, I.K.C., 2010. Mid- to late-Holocene paleoceanographic changes on the southeastern Brazilian shelf based on grain size records. The Holocene 20, 863–875. https://doi.org/10.1177/0959683610365936.

Hamanaka, N., Kan, H., Yokoyama, Y., Okamoto, T., Nakashima, Y., Kawana, T., 2012. Disturbances with hiatuses in high-latitude coral reef growth during the Holocene: correlation with millennial-scale global climate change. Glob. Planet. Chang. 80-81, 21–35. https://doi.org/10.1016/j.gloplacha.2011.10.004.

Hodell, D.A., Kanfoush, S., 2001. Abrupt cooling of Antarctic Surface Waters and sea ice expansion in the South Atlantic sector of the Southern Ocean at 5000 cal yr B.P. Quat. Res. 56, 191–198. https://doi.org/10.1006/qres.2001.2252.

Kleypas, J.A., 1996. Coral reef development under naturally turbid conditions: fringing reefs near Broad Sound, Australia, 1996. Coral Reefs 15, 153–167. https://doi.org/10.1007/BF01145886.

Krbetschek, M.R., Götze, J., Dietrich, A., Trautmann, T., 1997. Spectral information from minerals relevant for luminescence dating. Radiat. Meas. 27 (5–6), 695–748. https://doi.org/10.1016/S1350-4487(97)00223-0.

Kuffner, I.B., Toth, L.T., 2016. A geological perspective on the degradation and conservation of western Atlantic coral reefs. Conserv. Biol. 30 (4), 706–715. https://doi.org/10.1111/cobi.12725.

Leão, Z.M.A.N., Kikuchi, R.K.P., Ferreira, B.P., Neves, E.G., Sovierzoski, H.H., Oliveira, M.D.M., Maida, M., Correia, M.D., Johnsson, R., 2016. Brazilian coral reefs in a period of global change: A synthesis. Braz. J. Oceanogr. 64 (sp2), 97–116. https://doi.org/10.1590/S1679-875920160916064sp2.

Mariani, M., Fletcher, M., Dysdale, R.N., Saunders, K.M., Heijnis, H., Jacobsen, G., Zawadzki, A., 2017. Coupling of the intertropical convergence zone and southern hemisphere mid-latitude climate during the early to mid-Holocene. Geology 45 (12), 1083–1086. https://doi.org/10.1130/G39705.1.

Meyers, P.A., 2003. Application of organic geochemistry to paleolimnological recostructions: a summary of examples from Laurentian Great Lakes. Org. Geochem. 34, 261–289.

Mies, M., Francini-Filho, R.B., Zilberberg, C., Garrido, A.G., Longo, G.O., Laurentino, E., Güth, A.Z., Sumida, P.Y.G., Banha, T.N.S., 2020. South Atlantic coral reefs are major global warming refugia and less susceptible to bleaching. Front. Mar. Sci. 7, 514. https://doi.org/10.3389/fmars.2020.00514.

Montaggioni, L., 2005. History of Indo-Pacific coral reefs systems since the last glaciation: Development patterns and controlling factors. Earth Sci. Rev. 71 (1–2), 1–75. https://doi.org/10.1016/j.earscirev.2005.01.002.

Moreno, P.I., 2004. Millennial-scale climate variability in northwest Patagonia over the last 15 000 yr. J. Quat. Sci. 19 (1), 35–47. https://doi.org/10.1002/jqs.813.

Moura, R.L., Amado-Filho, G.M., Moraes, F.C., Brasileiro, P.S., Salomon, P.S., Mahiques, M.M., Bastos, A.C., Almeida, M.G., Silva, J.M., Araujo, B.F., Brito, F.P., Rangel, T.P., Silva Jr., J.M., Araujo, B.F., Brito, F.P., Rangel, T.P., Oliveira, B.C.V., Bahia, R.G., Paranhos, R.P.P., Dias, R.J.S., Siegle, E., Figueiredo Jr., A., Pereira, R.C., Leal, C.V., Hajdu, E., Asp, N.E., Gregoracci, G.B., Neumann-Leitão, S., Yager, P.L., Francini-Filho, R.B., Fróes, A., Campeão, M., Silva, B.S., Moreira, A.P.B., Oliveira, L., Soares, A.C., Araujo, L., Oliveira, N.L., Teixeira, J.B., Valle, R.B., Thompson, C.C., Rezende, C.E., Thompson, F.L., 2016. An extensive reef system at the Amazon River mouth. Sci. Adv. 2, e1501252 https://doi.org/10.1126/sciadv.1501252.

Murray, A.S., Wintle, A.G., 2000. Luminescence dating of quartz using an improved single-aliquot regenerative-dose protocol. Radiat. Meas. 32, 57–73. https://doi.org/10.1016/S1350-4487(99)00253-X.

Peluso, L., Tascheri, V., Nunes, F.L.D., Castro, C.B., Pires, D.O., Zilberberg, C., 2018. Contemporary and historical oceanographic processes explain genetic connectivity in a Southwestern Atlantic coral. Sci. Rep. 8, 2684. https://doi.org/10.1038/s41598-018-21010-y.

Pereira-Filho, G.H., Shintate, G.S.I., Kitahara, M.V., Moura, R.L., Amado-Filho, G.M., Bahia, R.G., Moraes, F.C., Neves, L.M., Francini, C.L.B., Gibran, F.Z., Motta, F.S., 2019. The southernmost Atlantic coral reef is off the subtropical island of Queimada Grande (24°S): Brazil. Bull. Mar. Sci. 95 (2), 277–287. https://doi.org/10.5343/bms.2018.0056.

Perry, C.T., Alvarez-Filip, L., 2018. Changing geo-ecological functions of coral reefs in the Anthropocene. Funct. Ecol. 33, 976–988. https://doi.org/10.1111/1365-2435.13247.

Perry, C.T., Larcombe, P., 2003. Marginal and non-reef-building coral environments. Coral Reefs 22 (4), 427–432. https://doi.org/10.1007/s00338-003-0330-5.

Perry, C.T., Smithers, S.G., 2011. Cycles of coral reef 'turn-on', rapid growth and 'turn-off' over the past 8500 years: a context for understanding modern ecological states and trajectories. Glob. Chang. Biol. 17, 76–86. https://doi.org/10.1111/j.1365-2486.2010.02181.x.

Peterson, R.G., Stramma, L., 1991. Upper-level circulation in the South Atlantic Ocean. Prog. Oceanogr. 26, 1–73.

Prescott, J.R., Stephan, L.G., 1982. The contribution of cosmic radiation to the environmental dose for thermoluminescence dating. In: Proceedings of the Second Specialist Seminar on Thermoluminescence Dating 6. Council of Europe, Strasbourg, pp. 17–25.

Toniolo, T.F., Giannini, P.C.F., Angulo, R.J., De Souza, M.C., Pessenda, L.C.R., Spotorno-Oliveira, P., 2020. Sea-level fall and coastal water cooling during the late Holocene in Southeastern Brazil based on vermetid bioconstructions. Mar. Geol. 428, 106281. https://doi.org/10.1016/j.margeo.2020.106281.

Toth, L.T., Aronson, R.B., Vollmer, S.V., Hobbs, J.W., Urrego, D.H., Cheng, H., Enochs, I. C., Combosch, D.J., Woesik, R.V., Macintyre, I.G., 2012. ENSO Drove 2500-year collapse of eastern Pacific coral reefs. Science 337, 81–84. https://doi.org/10.1126/science.1221168.

Toth, L.T., Kuffner, I.B., Stathkopoulos, A., Shinn, E.A., 2018. A 3,000-year lag between the geological and ecological shutdown of Florida's coral reefs. Glob. Chang. Biol. 24, 5471–5483. https://doi.org/10.1111/gcb.14389.

Vasconcelos, M.J.O., Leão, Z.M.A.N., Kikuchi, R.K.P., 2018. Coral reef growth pattern in eastern Brazil has not changed since the Holocene. Quater. Environ. Geosci. 09 (2), 49–61.

Vergés, A., Steinberg, P.D., Hay, M.E., Poore, A.G.B., Campbell, A.H., Ballesteros, E., Heck, L.K., Booth, D.J., Coleman, M.A., Feary, D.A., Figueira, W., Langlois, T., Marzinelli, E.M., Mizerek, T., Mumby, P.J., Nakamura, Y., Roughan, M., van Sebille, E., Gupta, A.S., Smale, D.A., Tomas, F., Werberg, T., Wilson, S., 2014. The tropicalization of temperate marine ecosystems: climate-mediated changes in herbivory and community phase shifts. Proc. Roy. Soc. 281, 20140846. https://doi.org/10.1098/rspb.2014.0846.

Vogel, J.S., Southon, J.R., Nelson, D.E., Brown, T.A., 1984. Performance of catalytically condensed carbon for use in accelerator mass spectrometry. Nucl. Instrum. Methods Phys. Res. Sect. B. Beam Interactions Mater. Atoms 5 (2), 289–293. https://doi.org/10.1016/0168-583X(84)90529-9.

Voigt, I., Chiessi, C.M., Piola, A.R., Henrich, R., 2015. Holocene changes in Antarctic intermediate water flow strength in the Southwest Atlantic. Paleogeogr. Paleoclimatol. Paleoecol. 463, 60–67. https://doi.org/10.1016/j.palaeo.2016.09.018.

Wainer, I., Prado, L.F., Khodri, M., Otto-Bliesner, B., 2014. Reconstruction of the South Atlantic Subtropical Dipole index for the past 12,000 years from surface temperature proxy. Sci. Rep. 4, 5291. https://doi.org/10.1038/srep05291.

Wentworth, C.K., 1922. A scale of grade and class terms for clastic sediments. J. Geol. 30, 377–392.

Wintle, A.G., Murray, A.S., 2006. A review of quartz optically stimulated luminescence characteristics and their relevance in single-aliquot regeneration dating protocols. Radiat. Meas. 41 (4), 369–391. https://doi.org/10.1016/j.radmeas.2005.11.001.

Woodroffe, C., Brooke, B., Linklater, M., Kennedy, D.M., Jones, B.G., Buchanan, C., Mleczko, R., Hua, Q., Zhao, J., 2010. Response of coral reefs to climate change: expansion and demise of the southernmost Pacific coral reef. Geophys. Res. Lett. 37, L15602 https://doi.org/10.1029/2010GL044067.